PLASMA SPRAYING: A TOOL TO PRODUCE METALLIC GLASS COATINGS

M. Gagné and C. Roy
Département de génie mécanique, Faculté des sciences appliquées
Université de Sherbrooke, Sherbrooke, Québec J1K 2R1, Canada.

ABSTRACT

Plasma arc spraying is used to produce metallic glass coatings onto mild steel substrates. Powder of a commercial alloy, "AMDRY 915", is amenable to achieve very dense and bonded amorphous coatings. The experimental conditions to obtain the alloy in the amorphous state, the temperature of crystallization and a number of engineering properties are discussed.

1. INTRODUCTION

The knowledge of amorphous structures such as those found in natural silica glasses have generated great interest in the fabrication and the properties of amorphous alloys. This class of materials known as metallic glasses exhibits unusual but very useful engineering properties. Such amorphous materials are produced by ultra-rapid coating of the order of 10^5 to 10^{10} $K.s^{-1}$ from the melt. Their structure is characterized by a diffuse halo x-ray diffraction pattern and by the absence of contrast in transmission election microscopy.

Since the original work by Klement and co-workers (1) in the early 1960's who developped new techniques for producing metallic glasses, numerous quenching methods (2) have been investigated including plasma spraying on cooled surfaces (3). Generally, the amorphous coatings obtained by the plasma process were porous and non adherent. Much improvement of the coating quality was necessary to achieve all the desired coating properties for functional mechanical components.

This paper describes a convenient method of depositing an amorphous coating on steel substrates by plasma-arc spray and it characterizes the coatings produced from powder of a brazing commercial alloy in terms of the mechanical properties and the thermal stability of the amorphous structure.

2. EXPERIMENTAL PROCEDURES

The powder composition of AMDRY-915 is as follows: Cr: 12-14%; Co: 10%; B: 2.2-3.2%; Si: 3.0-5.0%; C: 0.03% max; Ni: balance. The plasma spraying was accomplished in a small steel vessel in which the air was evacuated before the chamber was filled with inert gas. Coatings were sprayed onto mild steel substrates 40 mm x 20 mm x 5 mm. The surface to be sprayed was

sand blasted immediately before the deposition. During spraying a jet of inert gas was directed onto the freshly deposited layer to quench the coating at an estimated rate of $10^5 K.s^{-1}$. The deposition parameters used in this work are summarized in TABLE 1.

The nature of the coating and its morphology at the completion of each test were studied by x-ray diffractometry, scanning election and optical microscopy and vickers microhardness measurements. The coating/substrate interfacial adherence was determined following the standard test procedures (4). The wear rates, at 293 K, were then evaluated under sliding conditions with a pin-on disk configuration (5).

3. RESULTS AND DISCUSSION

Characteristics of the plasma sprayed coatings

Structure.- In the course of this study, the structural characteristics and properties of the coatings were compared with those of an amorphous ribbon of the same alloy obtained from "Alloy Metal Inc." (Troy, Michigan). Fig. 1 shows the diffraction patterns of the amorphous alloy obtained from the ribbon (top) and the sprayed coating in its amorphous (middle) and semi-amorphous state (bottom). The diffractogram of the amorphous structure of this alloy is typical of the "metglasses" diffraction patterns described in the literature (6). The representative spraying conditions for producing the coatings in a semi or fully amorphous structure are listed in TABLE 2. The first and foremost condition to obtain glass formation and retention in the coating is that the powder particles of the alloy must be completely melted in the plasma flame and remain in the liquid state until they reach the cold substrate. The occurence of unmelted and embedded particles in the coating creates porosity, reduces its adherence and increases the level of crystallinity. The quenching gas, nitrogen, was found as effective as helium to suppress crystallization of the freshly deposited layers. A more significant factor was the thermal energy build-up in the coating during the spraying process. As shown in TABLE 2, the longer the deposition time, or the thicker the coating, the more intensive had to be the gas flow rate to achieve the critical quench rate.

The transition temperatures and rate of crystallization of the amorphous alloy were monitored by taking measurements of hardness of the heat treated alloy. The influence of thermal annealing on the hardness is shown in Fig. 2. Slight irreversible changes on the diffraction pattern of the amorphous coating was observed after several hours annealing at 460°K. However concomitant variation in the hardness number were measured only after annealing at 530 K ; measurements of this parameter lack the precision to reliably detect changes in the structure. As is evident from Fig. 3, the sharpening of the diffraction peaks appeared following annealing 460 K and only when the annealing led to crystallization did one observe a normal diffraction pattern.

Coating thickness and stresses: Coatings that are deposited on

surfaces are usually in a state of mechanical stress and this effect becomes even more pronounced with hard coatings such as the present amorphous alloy. Internal stresses are often larger than the yield strength of the bulk material. Coating stresses vary also with coating thickness and it has been observed that thicker coating produces greater shear stresses at the interface. Whenever the shear stress is greater than the yield stress of the interface region, the coating separates from the substrate. By using this particular condition wherein the shear stress exceeds the yield stress on the critical values for determining the thickness of the coating, the optimum thickness can be determined. Using coatings of less than the optimum thickness will prevent separation of the films from the substrate. In the case of the amorphous coating, separation at the coating/substrate interface occurs in a coating of about 500 µm thick.

Adherence: Because of the extreme hardness of the amorphous coating, the degree of mechanical "keying" of the coating to the substrate is excellent. As indicated by the results in TABLE 3, the bonding strength reached a mean value as high as $> 30\ MN/m^2$; it was however strongly dependent upon the spraying conditions and the thickness of the coating and therefore the degree of crystallinity and the state of internal stress in the coating.

Coherence: The cohesive or bulk strength of the coating was evaluated by measuring the tensile strength of the coating removed from its substrate. As shown in TABLE 4, the amorphous coating exhibited a mean value very close to that of a tensile sample prepared from the amorphous ribbon. This data also shows that the cohesive strength of the coating was greatly affected by the presence of crystalline or unmelted particles within the coating. The influence of crystallization on the cohesive strength was also confirmed by comparing the tensile strength of amorphous and isothermally heat-treated tensile samples (TABLE 4). The amorphous coating fractured by decohesion within the amorphous grains leaving a vein pattern on the fracture surface, while the crystallized coating fractured much like a ductile material.

Sliding friction tests: TABLE 5 compares the wear coefficients for the alloy in the amorphous and crystalline state, mild steel and a chromite coating (Cr_2O_3). Under identical experimental conditions, the ceramic coating showed the lowest wear rate followed by the crystallized alloy coating. These results were unexpected because of the extreme hardness of the amorphous alloy. At this time, it is difficult to explain the exact source or reasons for the low wear resistance of the amorphous coating; however, two reasons can be offered:

1) Delamination of the particles around the periphery, as can be seen by observing the wear track, led initially to a high rate of formation of wear debris. This is consistent with a rapid wear rate initially followed by a wear resistance similar to the crystallized alloy.

2) The relatively low fatigue resistance of metglasses by comparison to crystalline material (7).

REFERENCES

(1) W. Klement, R.H. Willens and P. Duwez, Nature, Sept. 1960, p. 869.

(2) S. Takayama, Journal of Materials Science, vol. 11, 1976, pp 164-185.

(3) B.C. Giessen, N.M. Madhava, R.J. Murphy, R. Ray and J. Surrette, Metallurgical Transactions, vol. 8A, 1977, pp 364-366.

(4) T.J. Roseberry and F.W. Boulanger, A Plarma Flame Spray Handbook, Report # MT-043, Naval Ordnance Station, Louisville (1977).

(5) E. Rabinowicz, "Friction and Wear of Materials", edited by John Wiley and Sons (New-York, 1965).

(6) A. Schafer and G. Menzel, Thin Solid Films, vol. 52, 1978, pp 11-21.

(7) T. Masumoto and R. Maddin, Materials Science and Engineering, vol. 19, 1975, pp 1-24.

Melting of the particles	Plasma gas	Ar + 30% N_2
	Flow rate	28 l/min
	Power	18-20 kW
	Powder feed	35 g/min
	Powder gas	A (6 l/min)
Quenching	Gas	N_2 or He
	Flow rate	0-20 l/min

Table 1. Conditions of deposition

Power kW	Spraying time s	Adherence MN/m^2
18	10	16.1
20	10	13.1
20	10	16.4
19	5	21.0
20	5	21.9
20	5	27.6
20	5	29.3

Table 3. Adherence of amorphous coatings

Cooling gas	Spraying time s	Gas flow rate(l/min)	Vickers microhardness(mean value)(100g)	Structure
Nitrogen	5	5.8	1122	Amorphous
		8.6	1165	Amorphous
	10	3.4	986	Semi-amorphous
		4.7	820	Crystalline
		6.0	935	Semi-amorphous
		8.6	1286	Amorphous
Helium	5	5.6	745	Semi-amorphous
		6.3	852	Semi-amorphous
		8.6	905	Amorphous
		∿ 20	995	Amorphous
Without cooling	10	0	730	Crystalline
Amorphous ribbon	-	-	1035	Amorphous

Table 2. Crystallinity and hardness of the coatings

Material	Spraying condition	Coherence MN/m^2	Coherence after annealing
Coatings	P- 18 kW Semi-amorphous	388	-
	P- 20 kW Amorphous	719	322
Amorphous ribbon	-	714	350

Table 4. Coherence of the coatings

Material	Vickers Hardness	Wear constant
Amorphous coating	1000	5.4×10^{-5}
Amorphous ribbon	1000	5.6×10^{-5}
Crystalline coating	580	1.5×10^{-5}
Cr_2O_3	1350	10^{-6}
Mild steel	300	2.4×10^{-4}

Table 5. Wear resistance of different materials

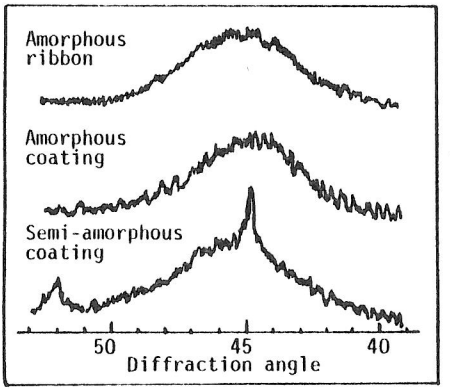

Figure 1.Diffraction patterns of amorphous materials.

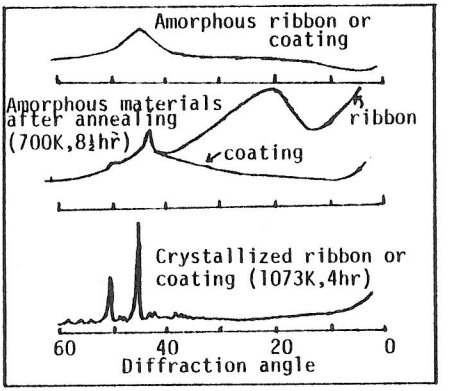

Figure 3.Diffraction patterns after annealings.

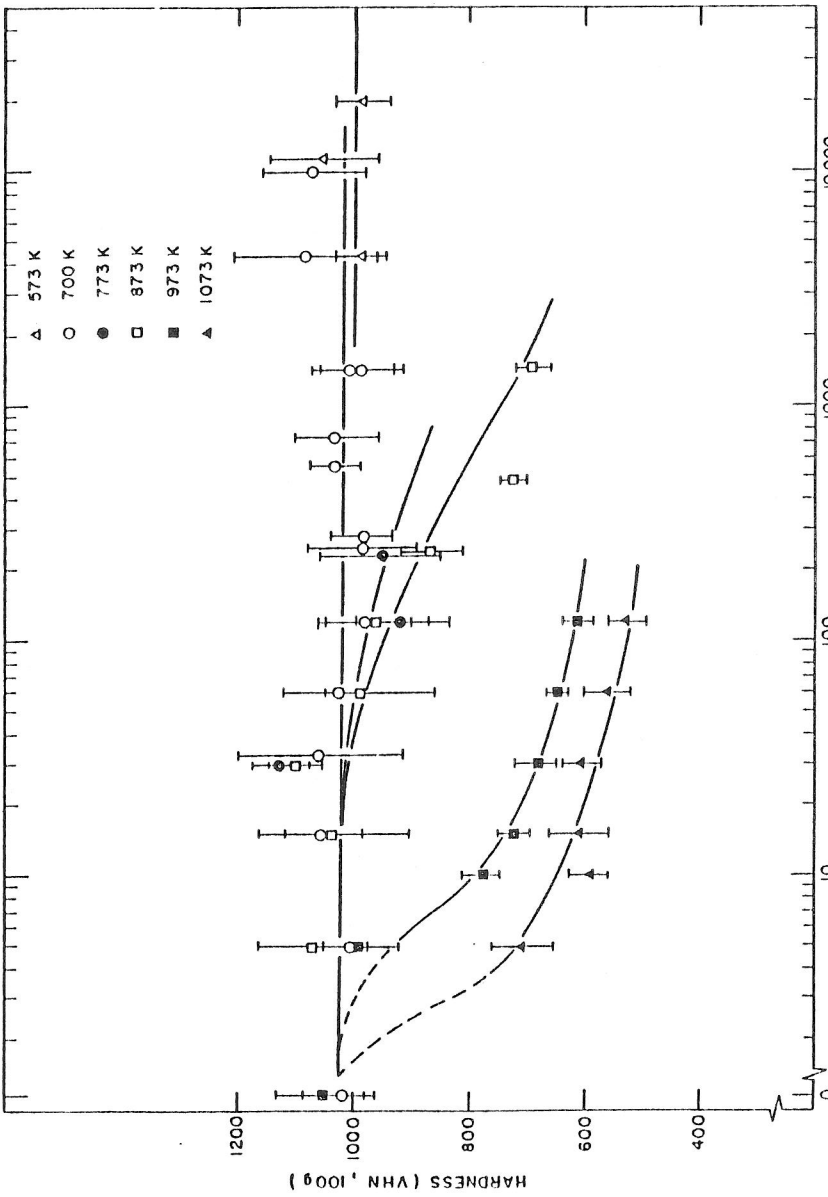

Figure 2. Hardness of heat-treated alloy